Upper Burst Error Bound for Atmospheric Correlated Optical Communications Using an Alternative Matrix Decomposition

Jurado-Navas, Antonio; Garrido-Balsellss, José María; Castillo-Vazquez, Miguel; Puerta-Notario, Antonio

Published in:
Computational Simulations and Applications

Link to article, DOI:
10.5772/24119

Publication date:
2011

Document Version
Publisher's PDF, also known as Version of record

20

Upper Burst Error Bound for Atmospheric Correlated Optical Communications Using an Alternative Matrix Decomposition

Antonio Jurado-Navas, José María Garrido-Balsells, Miguel Castillo-Vázquez and Antonio Puerta-Notario
Communications Engineering Department, University of Málaga
Campus de Teatinos
Málaga, Spain

1. Introduction

Atmospheric optical communication has been receiving considerable attention recently for use in high data rate wireless links (Arnon, 2003; Haas et al., 2002; Juarez et al., 2006; Zhu & Kahn, 2002). Considering their narrow beamwidths and lack of licensing requirements as compared to microwave systems, atmospheric optical systems are appropriate candidates for secure, high data rate, cost-effective, wide bandwidth communications. Furthermore, the atmospheric optical communications are less susceptible to the radio interference than radio-wireless communications. Moreover, free space optical (FSO) communication systems represent a promising alternative to solve the "last mile" problem, above all in densely populated urban areas. However, even in clear sky conditions, wireless optical links may experience fading due to the turbulent atmosphere. In this respect, inhomogeneities in the temperature and pressure of the atmosphere lead to variations of the refractive index along the transmission path. These random refractive index variations produce fluctuations in both the intensity and the phase of an optical wave propagating through this medium. Such fluctuations can lead to an increase in the link error probability limiting the performance of communication systems. In this particular scenario, the turbulence-induced fading is called scintillation.

If the receiving aperture size in these optical systems, D_0, can be made larger than the correlation length, d_0, then the received irradiance becomes a spatial average over the aperture area and the scintillation level measured by the detector begins to decrease. This effect is known as aperture averaging (Andrews & Phillips, 1998). Unfortunately, it could be neither practical nor desirable to satisfy this condition, especially in diversity receivers, so we will assume that $D_0 < d_0$ throughout this chapter.

Finally, weather-induced attenuation caused by rain, snow and fog can also degrade the performance of atmospheric optical communication systems in the way shown in (Al Naboulsi & Sizun, 2004; Muhammad et al., 2005), but are not considered in this chapter.

Spatial diversity reception is a good proposal in order to mitigate the adverse effect of the scintillation on the transmitted signal. Nevertheless, many researchers assume in a first approach that turbulence-induced fading is uncorrelated at each of the optical receivers

(Ibrahim & Ibrahim, 1996; Lee & Chan, 2004; Razavi & Shapiro, 2005). In order for this assumption to hold true, the spacing between receivers should be greater than the fading correlation length, what may be difficult to satisfy in practice because of the available physical space or due to the fact that the receiver spacing required for uncorrelated fading may exceed the beam diameter in power-limited links with well-collimated beams. For instance, with a propagation path length, L, of 1 km and an optical wavelength, λ, of 830 nm, the fading correlation length, approximated by $d_0 = (\lambda L)^{1/2}$ (Zhu & Kahn, 2002), would be of 2.89 cm. But, if $\lambda = 1550$ nm and $L = 10$ km, then the receiver spacing required for uncorrelated scintillation should be greater than 12.45 cm. In this respect, the spatial correlation is studied in detail in (Anguita et al., 2007), presenting a dependence on the turbulence parameter C_n^2 and, above all, a more remarkable dependence on the propagation distance and on the receiver aperture.

Thus, in (Jurado-Navas & Puerta-Notario, 2009), a complete model using an autorregresive (AR) model was presented to include correlated scintillations in simulations of free space optical links using multiple receivers. Obtained results showed a diversity gain penalty due to the impact of the spatial coherence which should not be ignored in many practical scenarios. Hence, the method proposed in (Jurado-Navas & Puerta-Notario, 2009) extended the applicability of the existing techniques (Beaulieu, 1999; Ertel & Reed, 1998), including the effect of the atmospheric dynamics in order to break the uniformity of the frozen-in hypothesis (Zhu & Kahn, 2002). This latter effect was incorporated by defining a factor, ρ_l, as follows:

$$\rho_l = \tau_0 / \tau_e \tag{1}$$

which represents the degree of randomness as effect of the dynamic evolution of the turbulence, with

$$\tau_0 = \frac{\sqrt{\lambda L}}{u_\perp} \tag{2}$$

being the turbulence correlation time, where λ is the optical wavelength, L is the propagation distance and $u_\perp$ the component of the wind velocity transverse to the propagation direction. Finally, τ_e is seen as the lifetime of turbulent eddies and it is directly depending on the turbulent kinetic energy dissipation rate, ϵ, that represents the atmospheric dynamics. as the rate of energy cascading from larger eddies to smaller ones.

The method is focused on a multichannel generalization of the autoregressive (AR) variate generation method in a way similar to (Baddour & Beaulieu, 2002) in order to satisfy Taylor's hypothesis of frozen turbulence. Therefore, m lognormal scintillation sequences are generated with specified second-order statistics: concretely, the cross-correlation function and the autocorrelation function between different sequences that let spatial and temporal correlations be interrelated.

2. Upper error bound in a simpler channel model

The AR model presented in (Jurado-Navas & Puerta-Notario, 2009) and commented above is computationally complex due to its inherent numerically ill-conditioned covariance matrix (Baddour & Beaulieu, 2002). In this chapter, we propose a space-time separable statistics model, extremely simple, to avoid such a problem, providing an excellent accurate upper burst error bound and with the advantage of a reduced computational time, for correlated atmospheric terrestrial links operating at optical wavelengths. This limit is heuristically corroborated after comparing the obtained performance using scintillation sequences derived

from (Jurado-Navas & Puerta-Notario, 2009) with different cross-correlation (CC) coefficient in terms of burst error rate, for an atmospheric optical link in the following two extreme situations: first, when a full accomplishment of the frozen turbulence hypothesis is assumed ($\rho_l \to 0$, $\tau_e \to \infty$); and second, when an unrealistic scenario is supposed owing to using only a space-time separable statistics model ($\rho_l \to 1$, $\tau_e \to \tau_0$), so that it can be assumed that the frozen-in turbulence is not incorporated to the system. Naturally, this latter situation is not corresponding to a real scenario, but it is presented in this paper as a benchmark in order to compare the obtained performance in burst error rate. In view of the results obtained by this latter scenario (shown through section 6 in this proposal of chapter) in comparison to the ones derived by using the first model (incorporating the frozen turbulence), it is concluded that a realistic upper error limit can be easily achieved with a high simplicity by using a space-time separable statistics model.
We must remark, however, that the space-time separable statistics model proposed here is an efficient approach that accomplishes more realistic performances when higher wind velocities are considered. In fact, this approach is based on coloring independent Gaussian sequences first between them and then in time in order to generate m log-normal random processes of scintillation. Evidently, such method is restricted to have cross-correlation functions that have the same time-dependencies as the autocorrelation functions, i.e., the obtained sequences have statistics that are space-time separable. Due to this fact, Taylor's hypothesis (Tatarskii, 1971) is not fully satisfied. For such a case, we must redirect readers to (Jurado-Navas & Puerta-Notario, 2009), where Taylor's frozen turbulence hypothesis is properly taken into account. Conversely, the frozen-in hypothesis is unquestionably an approximation and must fail as distance between receivers becomes large or in especial situations when there are both strong velocity fluctuations of the wind or long-range spatial correlations (Burghelea et al., 2005; Moore et al., 2005), or even in urban atmospheres, especially near or among roughness elements, where strong wind shear is expected to create high turbulent kinetic energy (Christen et al., 2007). Furthermore, in urban canopies and cloud streets up to $2-5$ times the average building height of such particular streets (Christen et al., 2007), the strong wind shear creates turbulence intensities that are tipically near the threshold where the hypothesis of frozen turbulence becomes inapplicable (Christen et al., 2007; Willis & Deardorff, 1976). In this fashion, difference in performance obtained from the realistic model presented in (Jurado-Navas & Puerta-Notario, 2009) and the upper bound performance proposed in this chapter are even closer to each other. Thus, the separable statistics model proposed here may be seen as a highly accurate upper error bound of the complete model detailed in (Jurado-Navas & Puerta-Notario, 2009), with the advantage of a reduced computational complexity in comparison to an AR method.

3. Turbulent atmospheric channel model

There is an extensive literature on the subject of the theory of line-of-sight propagation through the atmosphere (Andrews & Phillips, 1998; Andrews et al., 2000; Fante, 1975; Ishimaru, 1997; Strohbehn, 1978; Tatarskii, 1971). One of the most important works was developed by Tatarskii (Tatarskii, 1971). He supposed a plane wave that is incident upon the random medium (the atmosphere in this particular case). It is assumed an atmosphere having no free charges with a constant magnetic permeability. In addition, it is suppossed that the electromagnetic field has a sinusoidal time dependence (a monochromatic wave). Under these

circumstances, the vector wave equation becomes

$$\nabla^2\mathbf{E} + k^2 n^2(\mathbf{r})\mathbf{E} + 2\nabla\left(\mathbf{E}\cdot\nabla\log n(\mathbf{r})\right) = 0, \tag{3}$$

where $\mathbf{E}$ is the vector amplitude of the electric field, $k{=}2\pi/\lambda$ is the wave number of the electromagnetic wave with λ being the optical wavelength; whereas n is the atmospheric refractive index whose time variations have been suppressed, and being a random function of position, $\mathbf{r} = (x, y, z)$. The ∇ operator is the well-known vector derivative $(\partial/\partial x, \partial/\partial y, \partial/\partial z)$. Equation (3) can be simplified by imposing certain characteristics of the propagation wave. In particular, since the wavelength λ for optical radiation is much smaller than the smallest scale of turbulence, l_0, (Strohbehn, 1968) the maximum scattering angle is roughly $\lambda/l_0 \approx 10^{-4}$ rad. As a consequence, the last term on the left-hand side of Eq. (3) is negligible. Such a term is related to the change in polarization of the wave as it propagates (Strohbehn, 1971; Strohbehn & Clifford, 1967). This conclusion permit us to drop the last term and Eq. (3) then reduces to

$$\nabla^2\mathbf{E} + k^2 n^2(\mathbf{r})\mathbf{E} = 0. \tag{4}$$

Because Eq. (4) is easily decomposed into three scalar equations, one for each component of the electric field, $\mathbf{E}$, we may solve one scalar equation and ignore the vector character of the wave until the final solution. Therefore if we let $U(\mathbf{r})$ denote one of the scalar components that is transverse to the direction of propagation along the positive x-axis (Andrews & Phillips, 1998), then Eq. (4) may be replaced by the scalar stochastic differential equation

$$\nabla^2 U + k^2 n^2(\mathbf{r})U = 0. \tag{5}$$

The index of refraction, $n(\mathbf{r}){=}n_0 + n_1(\mathbf{r})$, fluctuates about the average value $n_0 = E[n(\mathbf{r})] \cong 1$, whereas $n_1(\mathbf{r}) \ll 1$ is the fluctuation of the refractive index from its free space value. Thus

$$\nabla^2 U + k^2(n_0 + n_1(\mathbf{r}))^2 U = 0. \tag{6}$$

For weak fluctuation, it is necessary to obtain an approximate solution of Eq. (6) for small n_1. Most of the literature since 1960 has followed the approach of using the so-called Rytov method, which substitutes U in a series:

$$U = \exp(\psi_0 + \psi_1 + \psi_2 + ...) = \exp(\psi). \tag{7}$$

In Eq. (7), ψ_1, ψ_2 are the first and second order complex phase perturbations, respectively, whereas ψ_0 is the phase of the optical wave in free space. The Rytov solution is widely used in line-of-sight propagation problems because it simplifies the procedure of obtaining both amplitude and phase fluctuations. From the Rytov solution, the wave equation becomes:

$$\nabla^2\psi + (\nabla\psi)^2 + k^2(n_0 + n_1(\mathbf{r}))^2 = 0. \tag{8}$$

This is a nonlinear first order differential equation for $\nabla\psi$ and is known as the Riccati equation. Consider now a first order perturbation, then

$$\psi(L, \mathbf{r}) = \psi_0(L, \mathbf{r}) + \psi_1(L, \mathbf{r}); \tag{9a}$$

$$n(\mathbf{r}) = n_0 + n_1(\mathbf{r}); \qquad n_0 \cong 1. \tag{9b}$$

Operating, assuming that $|\nabla\psi_1| \ll |\nabla\psi_0|$, due to $n_1(\mathbf{r}) \ll 1$, neglecting $n_1^2(\mathbf{r})$ in comparison to $2n_1(\mathbf{r})$, and equating the terms with the same order of perturbation, then the following expressions are obtained:

$$\nabla^2\psi_0 + (\nabla\psi_0)^2 + k^2 n_0^2(\mathbf{r}) = 0; \tag{10a}$$

$$\nabla^2\psi_1 + 2\nabla\psi_0\nabla\psi_1 + 2k^2 n_1(\mathbf{r}) = 0. \tag{10b}$$

The first one is the differential equation for $\nabla\psi$ in the absence of the fluctuation whereas turbulent atmosphere induced perturbation are found in the second expression. The resolution of Eq. (10b) is detailed in (Fante, 1975; Ishimaru, 1997). For the particular case of a monochromatic optical plane wave propagating along the positive x-axis, i.e., $U_0(L,\mathbf{r}) = \exp(jkx)$, this solution can be written as:

$$\psi_1(L,\mathbf{r}) = \frac{k^2}{2\pi}\iiint_V n_1(\mathbf{r}')\frac{\exp\left(jk\left[|\mathbf{r}-\mathbf{r}'| - |L-x'|\right]\right)}{|\mathbf{r}-\mathbf{r}'|}d^3\mathbf{r}', \tag{11}$$

where the position $(L,\mathbf{r})$ denotes a position in the receiver plane (at $x = L$) whereas $(x',\mathbf{r}')$ represents any position at an arbitrary plane along the propagation path. The mathematical development needed to solve Eq. (11) can be consulted in (Andrews & Phillips, 1998; Ishimaru, 1997). Furthermore, the statistical nature of $\psi_1(L,\mathbf{r})$ can be deduced in an easy way. Equation (11) has the physical interpretation that the first-order Rytov perturbation, $\psi_1(L,\mathbf{r})$ is a sum of spherical waves generated at various points $\mathbf{r}'$ throughout the scattering volume V, the strength of each sum wave being proportional to the product of the unperturbed field term U_0 and the refractive-index perturbation, n_1, at the point $\mathbf{r}'$ (Andrews & Phillips, 1998). Thus it is possible to apply the central limit theorem. According to such a theorem, the distribution of a random variable which is a sum of N independent random variables approaches normal as $N \to \infty$ regardless of the distribution of each random variable. Application of the central limit theorem to this integral equation leads to the prediction of a normal probability distribution for ψ. Since we can substitute $\Psi = \chi + jS$, where χ and S are called the log-amplitude and phase, respectively, of the field, then application of the central limit theorem also leads to the prediction of a Gaussian (normal) probability distribution for both χ and S, at least up to first order corrections (χ_1 and S_1).

Accordingly, under this first-order Rytov approximation, the field of a propagating optical wave at distance L from the source is represented by:

$$U = \exp(\psi) = U_0(L,\mathbf{r})\exp(\psi_1), \tag{12}$$

with $U_0(L,\mathbf{r})$ being the unperturbed portion of the field in the absence of turbulence. Hence, the irradiance of the random field shown in Eq. (12) takes the form:

$$I = |U_0(L,\mathbf{r})|^2\exp(\psi_1 + \psi_1^*) = I_0\exp(2\chi_1), \qquad [w/m^2] \tag{13}$$

where, from now onwards, we denote χ_1 as χ for simplicity in the notation. Hence,

$$I = I_0\exp(2\chi), \qquad [w/m^2]. \tag{14}$$

In Eq. (13), operator $*$ denotes the complex conjugate, $|U_0|$ is the amplitude of the unperturbed field and I_0 is the level of irradiance fluctuation in the absence of air turbulence that ensures that the fading does not attenuate or amplify the average power, i.e., $E[I] = |U_0|^2$. This may be thought of as a conservation of energy consideration and requires the choice of $E[\chi] = -\sigma_\chi^2$, as was explained in (Fried, 1967; Strohbehn, 1978), where $E[\chi]$ is the ensemble average of

log-amplitude, whereas σ_χ^2 is its variance depending on the structure parameter, C_n^2. With all of these expressions, we have modeled the irradiance of the random field, I, in the space at a single instant in time. Now, because the state of the atmospheric turbulence varies with time, the intensity fluctuations is also temporally correlated. Then, Eq. (14) can be expressed as:

$$I = \alpha_{sc}(t) \cdot I_0, \tag{15}$$

whereas $\alpha_{sc}(t) = \exp(2\chi(t))$ is the temporal behavior of the scintillation sequence and represents the effect of the intensity fluctuations on the transmitted signal. In Eq. (15), a space-to-time statistical conversion has been assumed by employing the well-known Taylor's hypothesis of frozen turbulence (Tatarskii, 1971; Taylor, 1938).
As analyzed before, and by the central limit theorem, the marginal distribution of the log-amplitude, χ, is Gaussian. Thus,

$$f_\chi(\chi) = \left(\frac{1}{2\pi\sigma_\chi^2}\right)^{1/2} \exp\left[-\frac{(\chi - E[\chi])^2}{2\sigma_\chi^2}\right]. \tag{16}$$

Hence, from the Jacobian statistical transformation (Papoulis, 1991),

$$f_I(I) = \frac{f_\chi(\chi)}{|\frac{dI}{d\chi}|}, \tag{17}$$

the probability density function of the intensity, I, can be identified to have a lognormal distribution typical of weak turbulence regime. Then:

$$f_I(I) = \left(\frac{1}{2I}\right)\left(\frac{1}{2\pi\sigma_\chi^2}\right)^{1/2} \exp\left[-\frac{(\ln I - \ln I_0)^2}{8\sigma_\chi^2}\right]. \tag{18}$$

Theoretical and experimental studies of irradiance fluctuations generally center around the scintillation index. It was evaluated in (Mercier, 1962) and it is defined as the normalized variance of irradiance fluctuations:

$$\sigma_I^2 = \frac{E[I^2]}{\left(E[I]\right)^2} - 1. \tag{19}$$

Hence it is possible to define the weak turbulence regimes as those regimes for which the scintillation index given in Eq. (19) is less than unity.
With all these considerations taken into account, an efficient channel model for FSO communications using intensity modulation and direct detection (IM/DD) was presented in (Jurado-Navas et al., 2007; 2011a) under the assumption of weak turbulence regime. For these systems, the received optical power, $Y(t)$, can be written as

$$Y(t) = \alpha_{sc}(t)X(t) + N(t), \tag{20}$$

being $X(t)$ the received optical power without scintillation; whereas $\alpha_{sc}(t) = \exp\left[2\chi(t)\right]$ is the temporal behavior of the scintillation sequence and represent the effect of the intensity fluctuations on the transmitted signal. To generate $\alpha_{sc}(t)$, a scheme based on a lowpass filtering of a random Gaussian signal, $z(t)$, is implemented as in (Jurado-Navas et al., 2007; 2011a). $\chi(t)$ is, as was explained above, the log-amplitude of the optical wave governed by Gaussian statistics with ensemble average $E[\chi]$ and variance σ_χ^2. Finally, the additive

white Gaussian noise, $N(t)$, is assumed to include any front-end receiver thermal noise as well as shot noise caused by ambient light much stronger than the desired signal. In the following section, we complete the scheme presented in (Jurado-Navas et al., 2007) to afford the inclusion of m correlated scintillation sequences approximating to the model introduced in (Jurado-Navas & Puerta-Notario, 2009).

4. Proposed approximation: space-time separable statistics channel model

As indicated in the last section, we can simplify the model proposed in (Jurado-Navas & Puerta-Notario, 2009) by an unrealistic but reasonably accurate space-time separable statistics model with a reduced computational load if it is compared with the complete model. Through this section, we develop the space-time separable statistics model.

4.1 Spatial diversity reception

When multiple receivers are considered, then, as shown in (Zhu & Kahn, 2002), the real symmetric auto-covariance matrix of the log-amplitude, $\mathbf{C}_{\boldsymbol{\chi}}=\{c_{\chi}(i,j)\}_{i,j=1}^{m}$, at m receivers in a plane transverse to the direction of propagation is given by:

$$\mathbf{C}_{\boldsymbol{\chi}} = \begin{pmatrix} \sigma_{\chi}^2 & \sigma_{\chi}^2\rho_{d_{12}} & \dots & \sigma_{\chi}^2\rho_{d_{1m}} \\ \sigma_{\chi}^2\rho_{d_{21}} & \sigma_{\chi}^2 & \dots & \sigma_{\chi}^2\rho_{d_{2m}} \\ \dots & \dots & \dots & \dots \\ \sigma_{\chi}^2\rho_{d_{m1}} & \sigma_{\chi}^2\rho_{d_{n2}} & \dots & \sigma_{\chi}^2 \end{pmatrix}_{m\times m} \tag{21}$$

where d_{ij} and $\rho_{d_{ij}}$ are the distance and its normalized CC coefficient respectively between points i and j in the receiver plane. In (Jurado-Navas & Puerta-Notario, 2009; Zhu & Kahn, 2002), a Gaussian spatial covariance function for the log-amplitude fluctuations is employed that approximates the theoretical covariance function resulting from Rytov theory.

In order to satisfy the hypothesis of frozen turbulence, we can adopt an AR model as in (Baddour & Beaulieu, 2002; Jurado-Navas & Puerta-Notario, 2009) as a possible solution. By doing so, the multichannel Yule-Walker equations are expressed as (Jurado-Navas & Puerta-Notario, 2009):

$$\begin{pmatrix} \mathbf{C}_{\boldsymbol{\chi}}[0]_{m\times m} & \mathbf{C}_{\boldsymbol{\chi}}[-1]_{m\times m} & \dots & \mathbf{C}_{\boldsymbol{\chi}}[-p+1]_{m\times m} \\ \mathbf{C}_{\boldsymbol{\chi}}[1]_{m\times m} & \mathbf{C}_{\boldsymbol{\chi}}[0]_{m\times m} & \dots & \mathbf{C}_{\boldsymbol{\chi}}[-p+2]_{m\times m} \\ \dots & \dots & \dots & \dots \\ \mathbf{C}_{\boldsymbol{\chi}}[p-1]_{m\times m} & \mathbf{C}_{\boldsymbol{\chi}}[p-2]_{m\times m} & \dots & \mathbf{C}_{\boldsymbol{\chi}}[0]_{m\times m} \end{pmatrix} \begin{pmatrix} \mathbf{A^H}[1]_{m\times m} \\ \mathbf{A^H}[2]_{m\times m} \\ \dots \\ \mathbf{A^H}[p]_{m\times m} \end{pmatrix} = - \begin{pmatrix} \mathbf{C}_{\boldsymbol{\chi}}[1]_{m\times m} \\ \mathbf{C}_{\boldsymbol{\chi}}[2]_{m\times m} \\ \dots \\ \mathbf{C}_{\boldsymbol{\chi}}[p]_{m\times m} \end{pmatrix}. \tag{22}$$

where $\mathbf{A}^H[k]$, $k = 1,2,...p$ are $m \times m$ matrices containing the multichannel AR model coefficients; whereas $\mathbf{C}_{\boldsymbol{\chi}}[j]$ is the covariance matrix evaluated in the 'j'-time instant. Then, the system of equations in Eq. (22) can be solved efficiently via the Levinson-Wiggins-Robinson algorithm (Kay, 1988). Once the $\mathbf{A}^H[k]$ coefficient matrices have been determined, we can obtain the $m \times m$ covariance matrix of the driving noise vector process of the AR model from:

$$\mathbf{C}_{\boldsymbol{w}} = \mathbf{C}_{\boldsymbol{\chi}}[0] + \sum_{k=1}^{p} \mathbf{C}_{\boldsymbol{\chi}}[-k]\mathbf{A}^H[k]. \tag{23}$$

Thus, after obtaining $\mathbf{C}_{\boldsymbol{w}} = E\{\boldsymbol{\omega}[n]\boldsymbol{\omega}[n]^T\}$, where the hermitian operator has been substituted by a transpose operator due to all the samples are real; the driving noise process, $\boldsymbol{\omega}[n]$,

can be accomplished as was indicated in (Baddour & Beaulieu, 2002). But first we need to compute the factorization $\mathbf{C}_{\boldsymbol{w}} = \mathbf{L}\mathbf{L}^T$. If $\mathbf{C}_{\boldsymbol{w}}$ is positive definite, a Cholesky decomposition is performable using the interval Cholesky method proposed in (Alefeld & Mayer, 1993) in order to include the desired correlation among scintillation sequences, with $\mathbf{L}$ being a lower triangular matrix (Beaulieu & Merani, 2000; Ertel & Reed, 1998). So, the driving process is then generated by the product $\boldsymbol{\omega}[n] = \mathbf{L}\mathbf{z}[n]$, where $\mathbf{z}[n]$ is an $m \times 1$ vector of independent zero mean Gaussian variates with unit variance and a autocorrelation function expressed as:

$$\mathbf{R}_{\boldsymbol{zz}} = E\{\mathbf{z}[n]\mathbf{z}^T[n]\} = \mathbf{I}_{\mathbf{m}}, \tag{24}$$

where $\mathbf{I}_{\mathbf{m}}$ is the 'm'-element identity matrix. Finally,

$$\boldsymbol{\chi}[n] = -\sum_{k=1}^{p} \mathbf{A}[k]\boldsymbol{\chi}[n-k] + \mathbf{w}[n]. \tag{25}$$

But if $\mathbf{C}_{\boldsymbol{w}}$ is not positive definite, then an alternative efficient decomposition algorithm that let the matrix be factorized was proposed in (Jurado-Navas & Puerta-Notario, 2009).

In addition, as said in the introduction, we can simplify the model proposed in (Jurado-Navas & Puerta-Notario, 2009) by an unrealistic but reasonably accurate space-time separable statistics model with a reduced computational load if it is compared with the complete model. Hence, we work directly with the covariance matrix, $\mathbf{C}_{\boldsymbol{\chi}}$, unlike the work proposed in (Jurado-Navas & Puerta-Notario, 2009), where the matrix to be decomposed is $\mathbf{C}_{\boldsymbol{w}}$.

Thus, when $\mathbf{C}_{\boldsymbol{\chi}}$ is positive definite, as in the Gaussian approximation employed in (Zhu & Kahn, 2002), a Cholesky decomposition is performable using the interval Cholesky method proposed in (Alefeld & Mayer, 1993) in order to include the desired correlation among scintillation sequences. Hence we find a lower triangular matrix $\mathbf{L}$ such that $\mathbf{C}_{\boldsymbol{\chi}} = \mathbf{L}\mathbf{L}^H$ in a similar way as in (Beaulieu & Merani, 2000; Ertel & Reed, 1998).

4.2 Constructing the coloring matrix

As we have already said, the AR model presented in (Jurado-Navas & Puerta-Notario, 2009) can be simplified by directly coloring independent Gaussian sequences first between them and then in time (space-time separable statistical model), avoiding the realization of the AR model. Obviously, this procedure is unrealistic because it implies that Taylor's hypothesis is not considered. However, numerical results obtained (and included through this chapter) show that this simplification behaves as a good approximation in terms of burst error rate.

Thus, we can directly consider the auto-covariance matrix of the log-amplitude, $\mathbf{C}_{\boldsymbol{\chi}}$. As commented before, when $\mathbf{C}_{\boldsymbol{\chi}}$ is positive definite, a Cholesky decomposition is performable by using the interval Cholesky method proposed (Alefeld & Mayer, 1993) in order to include the desired correlation among scintillation sequences. Hence we find a lower triangular matrix, $\mathbf{L}$, as a coloring matrix such that $\mathbf{C}_{\boldsymbol{\chi}} = \mathbf{L}\mathbf{L}^H$ in a similar way as in (Ertel & Reed, 1998).

Nevertheless, $\mathbf{C}_{\boldsymbol{\chi}}$ may not be positive definite so the Cholesky decomposition is not always feasible. Although any theoretical covariance matrix must be positive or, at least, semipositive definite, when such matrices are processed on a computer, small deviations from theory are introduced by the limits of floating point computations, inducing numeric inconsistencies. In this respect, there are no guarantees that the finite precision representation of the matrix can ensure positive definiteness, even more when the Cholesky algorithm is unstable for positive definite matrices that have one or more eigenvalues close to 0, as it is explained in

(Holton, 2004). In (Abramovich et al., 2001), the particular problem of non-positive definite matrices that arise from characterizing a realistic system is investigated in detail, showing that in 988 outcomes of their 1000 Monte Carlo trials, gave rise to a non-positive definite covariance matrix, although the corresponding "contracted" matrix may well be positive definite. In addition, in most practical situations the covariance matrix must be estimated from scintillation measurements (Monserrat et al., 2007; Moore et al., 2005) and outliers and other special situations as urban canopies may induce that correlation matrices derived from measurements are not always guaranteed to be positive definite, although a theoretical correlation matrix must always be.
In such cases, a real Schur decomposition is proposed (Golub & van Loan, 1996). Since the symmetric matrix $\mathbf{C}_{\boldsymbol{\chi}} \in \Re^{mxm}$, then there exists an orthogonal matrix, $\mathbf{Q} \in \Re^{mxm}$, such that

$$\mathbf{Q}^T \mathbf{C}_{\boldsymbol{\chi}} \mathbf{Q} = \mathbf{\Lambda} = \text{diag}(\lambda_1, ...\lambda_m) \tag{26}$$

as was shown in (Golub & van Loan, 1996), where superscript T denotes the transpose and $\lambda_i, \forall i = 1...m$, are the eigenvalues of $\mathbf{C}_{\boldsymbol{\chi}}$. In this case, we allow $\mathbf{C}_{\boldsymbol{\chi}}$ to have zero-eigenvalues. But however, as we will explain later, all the eigenvalues must be either zeros or positives. Unluckily, there will exist particular cases where $\mathbf{C}_{\boldsymbol{\chi}}$ might have any negative eigenvalue, as was indicated above. When this circumstance occurs, an adjustment of the Schur decomposition will be accomplished in order to obtain a positive semi-definite approximation, $\widetilde{\mathbf{C}}_{\boldsymbol{\chi}}=\{\widetilde{c}_{\chi}(i,j)\}$, to the original auto-covariance matrix of the log-amplitude, $\mathbf{C}_{\boldsymbol{\chi}}$, by minimizing the distance (Halmos, 1972):

$$\delta(\mathbf{C}_{\boldsymbol{\chi}}) = \min_{\widetilde{\mathbf{C}}_{\boldsymbol{\chi}}=\widetilde{\mathbf{C}}_{\boldsymbol{\chi}}^T \geq 0} \|\mathbf{C}_{\boldsymbol{\chi}} - \widetilde{\mathbf{C}}_{\boldsymbol{\chi}}\|, \tag{27}$$

where $\|\cdot\|$ represents the norm of the matrix $\mathbf{C}_{\boldsymbol{\chi}} - \widetilde{\mathbf{C}}_{\boldsymbol{\chi}}$. We distinguish two main situations (Jurado-Navas & Puerta-Notario, 2009) corresponding to minimize the Frobenius norm (Golub & van Loan, 1996) or the the p-norms (with $p = 1, 2, \infty$), respectively. In both cases, we can substitute the diagonal matrix $\mathbf{\Lambda}$ by a resulting matrix written as $\mathbf{R} = \mathbf{\Lambda} + \mathbf{Y}$, where $\mathbf{Y}$ is a perturbation matrix obtained after minimizing Eq. (27) in any of the two situations mentioned above. After that, and for any of these two scenarios, we can form the coloring matrix, $\mathbf{K}$, as $\mathbf{K} = \mathbf{Q}(\mathbf{R})^{\mathbf{1/2}}$ in order to generate the correlated log-normal scintillation samples. Here it is shown why we need that $\mathbf{C}_{\boldsymbol{\chi}}$ were approximated by a positive semi-definite matrix if any eigenvalue of $\mathbf{C}_{\boldsymbol{\chi}}$ is negative. In this case,

$$\widetilde{\mathbf{C}}_{\boldsymbol{\chi}} = \mathbf{K}\mathbf{K}^T = \left(\mathbf{Q}\left(\mathbf{\Lambda} + \mathbf{Y}\right)^{1/2}\right)\left(\mathbf{Q}\left(\mathbf{\Lambda} + \mathbf{Y}\right)^{1/2}\right)^T = \mathbf{Q}\mathbf{R}\mathbf{Q}^T; \tag{28}$$

however, if all eigenvalues of $\mathbf{C}_{\boldsymbol{\chi}}$ are positive, then

$$\mathbf{C}_{\boldsymbol{\chi}} = \mathbf{K}\mathbf{K}^T = \left(\mathbf{Q}\mathbf{\Lambda}^{1/2}\right)\left(\mathbf{Q}\mathbf{\Lambda}^{1/2}\right)^T = \mathbf{Q}\mathbf{\Lambda}\mathbf{Q}^T. \tag{29}$$

Let us see these two scenarios in detail:

4.2.1 General scenario

If any λ_i in $\mathbf{\Lambda}$ is negative, then we can approximate the matrix $\mathbf{\Lambda}$ substituting every negative eigenvalue for 0. The resulting matrix may be written as

$$\mathbf{R} = \mathbf{\Lambda} + \mathbf{Y}, \tag{30}$$

where $\mathbf{Y}$ is a diagonal perturbation matrix with diagonal elements, $\{v_i\}_{i=1}^{m}$, of

$$v_i = \begin{cases} -\lambda_i, \text{ if } \lambda_i < 0; \\ 0, \quad \text{if } \lambda_i \geq 0; \end{cases} \qquad \forall \mathrm{i} = 1, 2...\mathrm{m}. \tag{31}$$

In this case, the approximation $\widetilde{\mathbf{C}}_{\boldsymbol{\chi}} = \mathbf{QRQ}^T$ is proven to optimize the Frobenius norm if $(v_i + \lambda_i) \to 0$, and with the constraint of having a positive semi-definite solution matrix, $\widetilde{\mathbf{C}}_{\boldsymbol{\chi}}$; where the Frobenius norm is detailed in (Golub & van Loan, 1996) and represented by

$$\|\mathbf{A}\|_F = \sqrt{\sum_{i=1}^{m}\sum_{j=1}^{m} |\mathrm{c}_{\chi}(\mathrm{i,j}) - \widetilde{\mathrm{c}}_{\chi}(\mathrm{i,j})|^2}. \tag{32}$$

4.2.2 Specific scenario

If instead of employing the Frobenius norm, the expression (27) is optimized for the relevant $2-$norm matrix defined as:

$$\|\mathbf{C}_{\boldsymbol{\chi}} - \widetilde{\mathbf{C}}_{\boldsymbol{\chi}}\|_2 = \sqrt{\rho\left\{(\mathbf{C}_{\boldsymbol{\chi}} - \widetilde{\mathbf{C}}_{\boldsymbol{\chi}})^H (\mathbf{C}_{\boldsymbol{\chi}} - \widetilde{\mathbf{C}}_{\boldsymbol{\chi}})\right\}}, \tag{33}$$

then we can obtain a new and different solution for the same problem. In equation (33), $\rho\left\{(\mathbf{C}_{\boldsymbol{\chi}} - \widetilde{\mathbf{C}}_{\boldsymbol{\chi}})^H (\mathbf{C}_{\boldsymbol{\chi}} - \widetilde{\mathbf{C}}_{\boldsymbol{\chi}})\right\}$ is the spectral radius of the matrix $(\mathbf{C}_{\boldsymbol{\chi}} - \widetilde{\mathbf{C}}_{\boldsymbol{\chi}})^H (\mathbf{C}_{\boldsymbol{\chi}} - \widetilde{\mathbf{C}}_{\boldsymbol{\chi}})$, defined as the supremum among the absolute values of its eigenvalues. Obviously, the hermitian operator can be substituted by a transpose operator since the samples are all real. As a characteristic feature, optimizing the $2-$norm entails, in general, multiple solutions for $\widetilde{\mathbf{C}}_{\boldsymbol{\chi}}$, as a main difference with respect to the previous situation.

Again, we define $\mathbf{R} = \boldsymbol{\Lambda} + \mathbf{Y}$, being $\mathbf{Y}$ the perturbation matrix. One of the possible solutions for $\mathbf{Y}$ that let $\mathbf{R}$ be a semi-definite positive matrix is obtained by constructing $\mathbf{Y}$ as a diagonal matrix whose elements are defined as $\{v_i = -\lambda \quad \forall\, \mathrm{i} = 1...m\}$, being λ the highest among the absolute values of the negative eigenvalues of the matrix $\mathbf{C}_{\boldsymbol{\chi}}$. Obviously, as in the above scenario, we obtain greater accuracies when smaller magnitudes were summed to $\boldsymbol{\Lambda}$. The limit, again, is the necessary magnitude that let the negative eigenvalue be canceled and so, $\mathbf{C}_{\boldsymbol{\chi}}$ were approximated to the closest positive semi-definite matrix. In this way, this second scenario is proven to minimize the p-norms (with $p = 1, 2, \infty$) since $\mathbf{Y}$ is a diagonal matrix in which all its entries have the same value. These norms can be consulted in (Golub & van Loan, 1996).

As final comment to this second scenario, we can remark that the great resemblance obtained between $\mathbf{C}_{\boldsymbol{\chi}}$ and $\widetilde{\mathbf{C}}_{\boldsymbol{\chi}}$ is based on the orthogonality of the rows of the matrix $\mathbf{Q}$. For example, suppose that the covariance matrix is non-positive definite expressed as

$$\mathbf{C}_{\boldsymbol{\chi}} = \begin{pmatrix} 0.100 & 0.079 & 0.010 \\ 0.079 & 0.100 & 0.079 \\ 0.010 & 0.079 & 0.100 \end{pmatrix}_{3\times 3}. \tag{34}$$

Hence, applying the decomposition shown in scenario 2, we obtain that $\widetilde{\mathbf{C}}_{\boldsymbol{\chi}} = \mathbf{C}_{\boldsymbol{\chi}}$, except for the principal diagonal, that now is $\widetilde{c}_{\chi}(i,i) = 0.106\ \forall i = 1...3$, i.e.:

$$\mathbf{C}_{\boldsymbol{\chi}} = \begin{pmatrix} 0.106 & 0.079 & 0.010 \\ 0.079 & 0.106 & 0.079 \\ 0.010 & 0.079 & 0.106 \end{pmatrix}_{3\times 3}. \tag{35}$$

Finally, if the original auto-covariance matrix is not symmetric, then the Schur decomposition is written as

$$\mathbf{C}_{\boldsymbol{\chi}} = \mathbf{Q}\mathbf{U}\mathbf{Q}^T, \tag{36}$$

where $\mathbf{U} \in \Re^{nxn}$ is upper triangular as was shown in (Golub & van Loan, 1996). In these circumstances, we can form the matrix $\mathbf{\Lambda}$ taking into account solely the diagonal elements of $\mathbf{U}$ before applying any of the two approximations proposed in this paper.

4.3 Generation of turbulent spatially-correlated channels

Now we can form the coloring matrix, $\mathbf{K} \in \Re^{mxm}$

$$\mathbf{K} = \mathbf{Q}\left(\mathbf{\Lambda} + \mathbf{Y}\right)^{1/2}, \tag{37}$$

in order to generate the correlated log-normal scintillation samples. Then, it follows that (Jurado-Navas & Puerta-Notario, 2009)

$$\mathbf{K}\mathbf{K}^T = \left(\mathbf{Q}\left(\mathbf{\Lambda} + \mathbf{Y}\right)^{\frac{1}{2}}\right)\left(\mathbf{Q}\left(\mathbf{\Lambda} + \mathbf{Y}\right)^{\frac{1}{2}}\right)^T = \mathbf{Q}\left(\mathbf{\Lambda} + \mathbf{Y}\right)^{\frac{1}{2}}\left(\left(\mathbf{\Lambda} + \mathbf{Y}\right)^{\frac{1}{2}}\right)^T\mathbf{Q}^T = \mathbf{Q}(\mathbf{\Lambda} + \mathbf{Y})\mathbf{Q}^T = \widetilde{\mathbf{C}}_{\boldsymbol{\chi}}, \tag{38}$$

as was shown in Eq. (28), where $\widetilde{\mathbf{C}}_{\boldsymbol{\chi}} = \mathbf{C}_{\boldsymbol{\chi}}$ if there does not exist any negative element in diagonal matrix $\mathbf{\Lambda}$ written in (26). Equation (37) shows why we need that $\mathbf{C}_{\boldsymbol{\chi}}$ were approximated by a positive semi-definite matrix if any eigenvalue of $\mathbf{C}_{\boldsymbol{\chi}}$ is negative even when a Schur decomposition could be always accomplished if the starting matrix is squared. Next, define $\mathbf{Z} = \left[z^{(1)}[n],\, z^{(2)}[n],\, \ldots\, z^{(m)}[n]\right]^T$ as a set of uncorrelated white Gaussian signals. Its correlation matrix, R_{ZZ}, is given by

$$\mathbf{R}_{\mathbf{ZZ}} = E\{\mathbf{z}[n]\mathbf{z}^T[n]\} = \mathbf{I}_{\mathbf{m}}, \tag{39}$$

where $\mathbf{I}_{\mathbf{m}}$ is the 'm'-element identity matrix. By calculating $\mathbf{w}[n] = \mathbf{K}\mathbf{z}[n]$, being

$$\mathbf{w}[n] = \left[w^{(1)}[n],\, w^{(2)}[n],\, \ldots\, w^{(m)}[n]\right]^T, \tag{40}$$

the desired auto-covariance matrix of the log-amplitude fluctuations is obtained since

$$E\{\mathbf{w}[n]\cdot\mathbf{w}^T[n]\} = E\{\mathbf{K}\cdot\mathbf{z}[n]\cdot\mathbf{z}[n]^T\cdot\mathbf{K}^T\} = \mathbf{K}\mathbf{K}^T = \widetilde{\mathbf{C}}_{\boldsymbol{\chi}}. \tag{41}$$

Furthermore, every $w^{(i)}[n], \forall i = 1...m$ in Eq. (40) remains statistically Gaussian so it is possible to filter them in the way proposed in (Jurado-Navas et al., 2007) in order to obtain $\alpha_{sc}^{(i)}(t)$ for each of the m receivers. The filter employed in each branch is the Gaussian filter shown in (Jurado-Navas et al., 2007). Therefore, the output signal of these filters is the log-amplitude fluctuations, $\chi^{(i)}(t)\ \forall i = 1...m$, for each receiver. These outputs exhibit a Gaussian probability density function and have the desired covariance matrix, $\mathbf{C}_{\boldsymbol{\chi}}$, among sequences but without its inherent time-dependencies that would be enforced by the frozen-in hypothesis, according to the space-time separable statistics approximation imposed in this chapter. Next, its probability density function is converted from Gaussian to lognormally distributed, generally accepted for the irradiance fluctuations under weak turbulence conditions. Figure 1 shows clearly the overall process.

In this respect, it is possible to employ the same procedure explained in this paper but knowing that, instead of the log-normal employed here, a Beckman probability density much

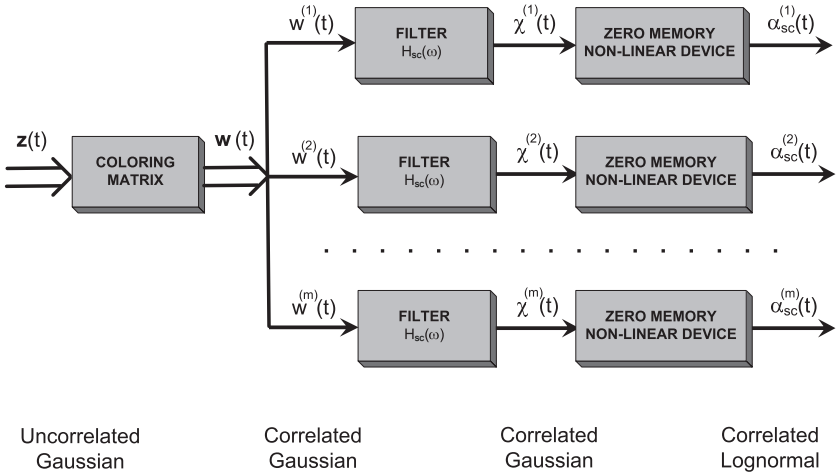

Fig. 1. Block diagram representing the generation of 'm' equal power log-normal scintillation sequences with a space-time separable statistics approximation.

more accurately reflects the statistics of the intensity scintillations (Hill & Frehlich, 1997) if Rytov variance increases even beyond the limits of the weak turbulence regime; or even the recently discovered Málaga probability density function (Jurado-Navas et al., 2011b), also very accurate with the statistics of the intensity scintillations.

5. System model

To study the performance of different values of spatial CC coefficients, ρ_{ij}, between points i and j in the receiver plane, intensity modulation and direct detection (IM/DD) links are assumed operating at a laser wavelength of 830 nm through a 250 m horizontal path at a bit rate of 50 Mbps. Assume three receivers in the system, where a conventional equal-gain combining (EGC) of diversity branches is implemented. Figure 2 shows the temporal behavior of correlated scintillation sequences for these three different receivers with a CC coefficient of $\rho_{12} = 0.56$ and $\rho_{13} = 0.1$ respectively, for this two extreme scenarios: an AR model, as in (Jurado-Navas & Puerta-Notario, 2009), and the space-time separable statistics approximation employed in this chapter. The component of the wind velocity, $u_{\perp}$, transverse to the propagation direction is fixed to $u_{\perp} = 20$ m/s, where ρ_{ij} is the normalized CC coefficient between points i and j in the receiver plane. Clearly, the election of a 20 m/s wind speed in this chapter will not be by far the typical operational scenario unless one of the terminals is in motion or the optical link is settled in particular geographical locations specifically affected by strong wind (Campins et al., 2007); but, however, such value is selected for numerical convenience so that we can work with a lower computational cost, because the total amount of samples needed to obtain a scintillation sequence with the desired lognormal statistics is smaller than using more conventional values for $u_{\perp}$, but letting us extract the same conclusions than employing a standard velocity.

Hence, a different temporal variability is shown in Figure 2 (a) and (b) for the EGC-combined scintillation sequence, being faster for the obtained sequence from a space-time separable statistics model. This different variability must have a different repercussion in the associated burst error rate curves, as shown below, where we followed Deutsch and Miller's

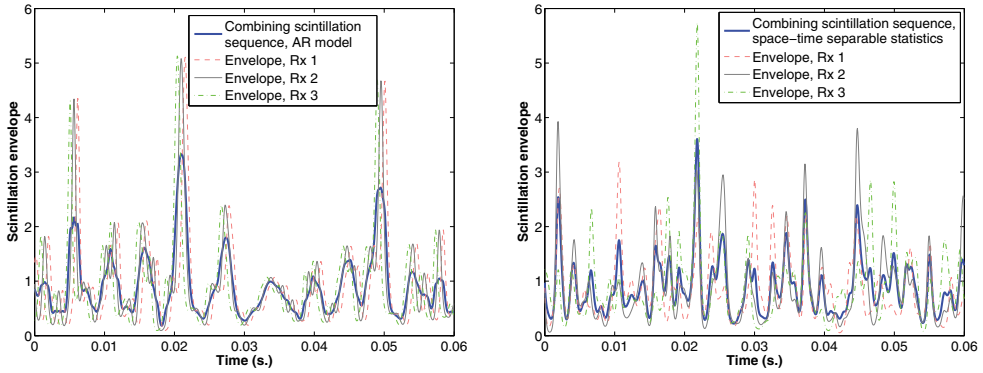

(a) (b)

Fig. 2. Scintillation sequences generated from (a) an AR model; (b) a space-time separable statistics model, for a 3-receivers system. The EGC sequence is displayed in thicker solid line.

(Deutsch & Miller, 1981) definition of a burst error with lengths of 192, and 64 bits, not containing more than 4 consecutive correct bits ($L_b = 5$, as explained in (Deutsch & Miller, 1981)) any sequence of burst error.
Then, pulses with on-off keying format (OOK) and Gaussian shape (OOK-GS) with a duty cycle (d.c.) of 100% are adopted, where identical average optical power is transmitted for every simulated case representing the reference condition to establish the comparative analysis (Jurado-Navas et al., 2010). All these features are included in the system model, where its remarkable elements are: first, the channel model presented in (Jurado-Navas et al., 2007) corresponding to a turbulent atmospheric environment, but included in a m-branch reception as in (Jurado-Navas & Puerta-Notario, 2009), which represent the m different correlated turbulence-induced fadings at each of the optical receivers; secondly, a 500 kHz three-pole Bessel highpass filter for natural and artificial light adverse effects suppression; and, thirdly, a five-pole, Bessel, lowpass filter employed as a matched filter. As said above, a conventional EGC is implemented whereas the detection procedure considered is a maximum likelihood (ML) detection. The receivers employed in this paper are point receivers whereas the weather-induced attenuation is neglected so that we concentrate our attention on turbulence effects. Furthermore, the atmospheric-induced beam spreading that causes a power reduction at the receiver is also neglected because, in our specific case, we are considering a terrestrial link where beam divergence is typically on the order of 10 μRad. This temporal spreading may be considered at high data rate, as in (Jurado-Navas et al., 2009), particularly when operating in special scenarios where dust particles are likely present.

6. Numerical results

The first set of results are displayed in Figure 3 for a three-receivers system and for $\sigma_\chi^2 = 0.25$ and $\sigma_\chi^2 = 0.1$, where the CC coefficients between scintillation sequences are:

- ρ_{12}=ρ_{21}=ρ_{23}=ρ_{32}=0.30 and ρ_{13}=ρ_{31}=0.008
- ρ_{12}=ρ_{21}=ρ_{23}=ρ_{32}=0.56 and ρ_{13}=ρ_{31}=0.1
- ρ_{12}=ρ_{21}=ρ_{23}=ρ_{32}=0.79 and ρ_{13}=ρ_{31}=0.1

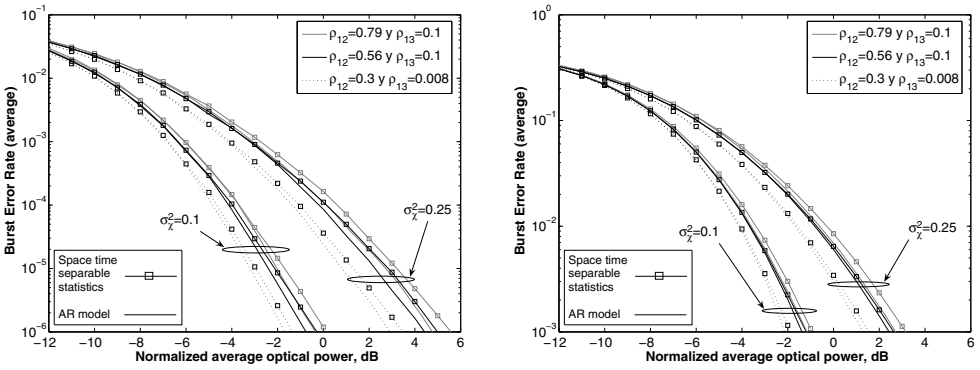

Fig. 3. Burst error rate of a system with 3 receivers versus normalized average optical power using OOK and ML detection, for different values of ρ_{ij} and σ_χ^2, with a wind velocity of $u_\perp = 20$ m/s. The burst error length is established to (a) 192 bits, (b) 64 bits.

where, for the last case, we need to calculate the positive semidefinite approximation to the original autocovariance matrix of the log-amplitude, as was explained in this chapter for a space-time separable statistics model and in (Jurado-Navas & Puerta-Notario, 2009) for an AR model, because the original autocovariance matrix is not positive definite and can not be factorized by a classical Cholesky decomposition method. Anyway, the obtainment of the covariance matrix involving the process in both scenarios must be factored to finally build the set of Gaussian log-amplitude sequences measured at the different receivers in the system. As shown in Figure 3, there only exists a slight difference (approx. 1–2 optical dB at a burst error rate of 10^{-6} for a length of burst of 192 bits) between the obtained performance from the AR model ($\rho_l \to 0$) and the one obtained from the space-time separable statistics model ($\rho_l \to 1$) proposed in this paper. In fact, this latter model offers an accurate upper error bound for the link performance in terms of burst error rate. Similar conclusions may be deduced from the curves simulated with a length of burst of 64 bits. Nevertheless, from this Figure 3, we can observe that diversity reception can improve the performance of the link, but a gain penalty is shown when the CC coefficient between two receivers is high, especially if the log-amplitude variance, σ_χ^2, is larger. This fact can be a plausible reason to include the consideration of the spatial channel coherence as a key factor to fully evaluate the performance of atmospheric optical communication systems.

Furthermore, Figure 4 shows some obtained results when the CC coefficient has been established to ρ_{12}=ρ_{21}=ρ_{23}=ρ_{32}=0.56 and ρ_{13}=ρ_{31}=0.1, for a length of burst of 192 bits. Figure 4 (a) represents the behavior of an OOK-GS format with a 100% d.c. for different intensities of turbulence. As in Figure 3, the difference in performance is not significant for the two extreme scenarios studied in this chapter. Only when the log-amplitude variance, σ_χ^2, is getting stronger, such difference between scenarios gets higher, for instance, from 0.17 to 1.2 optical dB for $\sigma_\chi^2 = 0.01$ and $\sigma_\chi^2 = 0.5$ respectively at a burst error rate of 10^{-6}.

Next, the pair of curves displayed for $\sigma_\chi^2 = 0.15$ are taken as a reference in Figure 4 (b). To show the superiority of the different pulse, we analyze the performance of Gaussian pulse shapes in terms of the peak-to-average optical power ratio (PAOPR) and burst error rate. Note that the PAOPR is a favorable characteristic in IM/DD infrared links due to

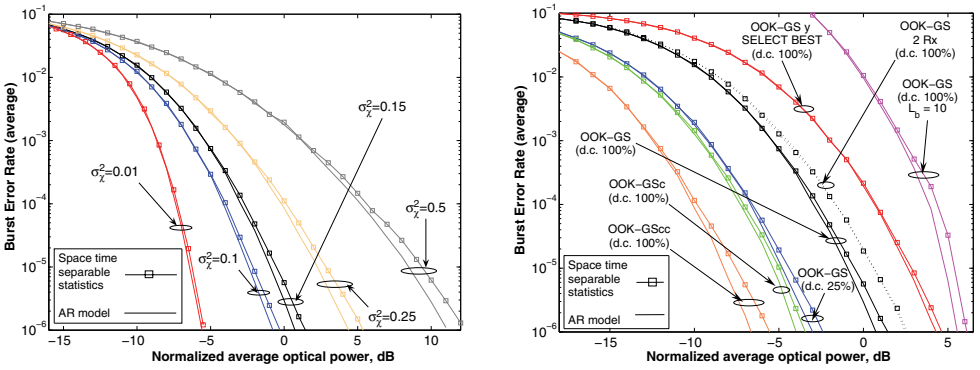

Fig. 4. Burst error rate of a system with 3 receivers versus normalized average optical power using OOK format, EGC and ML detection, assuming $\rho_{12} = 0.56$ and $\rho_{13} = 0.1$, being $u_\perp = 20$ m/s, whereas the burst error length is established to 192 bits. An OOK-GS format with d.c. of 100% is represented in (a), for different values of σ_χ^2. Different transmission formats have been displayed in (b) for $\sigma_\chi^2 = 0.15$.

the inherent cuadratic response of the optical detector and the average power constraints previously mentioned (Jurado-Navas et al., 2010). For this reason, we use the increase in PAOPR as a figure of merit to compare the different pulses performance, taking into account that a burst error rate analysis must be performed to take into account the temporal variability of different combined sequences and verify that the increase in distortion of shorter pulses does not counteract the PAOPR benefits. In this sense, pulses have been modified by varying their statistics of the amplitude sequence with the purpose of increasing this PAOPR, for example with a reduced d.c. of 25%; or even using OOK-GS formats with memory to avoid the appearance of more than one pulse in sets of two (OOK-GSc) and three (OOK-GScc) consecutive symbol periods (Jurado-Navas et al., 2010) but maintaining the average optical power at the same constant level in all cases. The inclusion of memory on OOK formats allows to increase the separation in burst error rate between the AR model and space-time separable statistics one. The same conclusion may be deduced when different combining techniques are employed (an EGC technique offers more distant results than a select best scheme); or when a different number of receivers make part of the system, or even when the definition of a burst error is modified allowing to contain, for instance, up to 9 consecutive correct bits any sequence of burst error, as displayed in Figure 4 (b). Thus, when we get more complicated the transmission format with the aim of obtaining a better performance, then the difference in burst error rate between considering (AR model) or not (separable statistics model) the frozen-in hypothesis is getting increased in a more meaningful way, but offering this separable statistics model a reasonably accurate upper error limit in terms of burst error rate in all simulated cases with a reduced computational load.

7. Concluding remarks

When technical specifications may not permit sufficient receiver spacing, scintillation sequences may be spatially correlated. For these cases, an efficient method for generating an

accurate approximation of 'm' equal power log-normal scintillation sequences with any CC coefficient is proposed in this paper, overcoming the restrictions of a Cholesky decomposition. Hence, the AR-model proposed in (Jurado-Navas & Puerta-Notario, 2009) and its inherent numerically ill-conditioned covariance matrix (Baddour & Beaulieu, 2002) may be avoided in many cases when calculating burst error rate curves due to the difference between the two extreme scenarios studied in this chapter is usually limited to approximately 2 dB at a burst rate of 10^{-6}. In this sense, the space-time separable statistics model proposed here can be used to consider spatial correlations among scintillation sequences without fear of making big mistakes and with the advantage of a reduced computational time. Thus, such separable statistics model may be seen as a highly accurate upper error bound of the whole model detailed in (Jurado-Navas & Puerta-Notario, 2009).

8. Acknowledgment

This work was supported by the Spanish Ministerio de Ciencia e Innovación, Project TEC2008-06598.

9. Nomenclature

$\mathbf{A}[k]$	$m \times m$ matrices containing the multichannel AR model coefficients.
C_n^2	Refractive-index structure parameter.
$\mathbf{C_w}$	Covariance matrix of the driving noise vector process of an AR model.
$\mathbf{C}_\chi$	Covariance matrix of the log-amplitude scintillation.
$\mathbf{C}_\chi[j]$	Covariance matrix of the log-amplitude scintillation evaluated in the j-time instant.
$\widetilde{\mathbf{C}}_\chi$	Positive semi-definite approximation of $\mathbf{C}_\chi$.
d_0	Correlation length of intensity fluctuations.
d_{ij}	Distance between points i and j in the receiver plane (m).
$\mathbf{E}$	Vector amplitude of the electric field.
$f_\chi(\chi)$	Probability density function of random log-amplitude scintillation.
$f_I(I)$	Probability density function of intensity fluctuations (=$f_{\alpha_{sc}}(\alpha_{sc})$).
I	Irradiance of the random field.
I_0	Level of irradiance fluctuation in the absence of air turbulence.
$\mathbf{I_m}$	m-element identity matrix.
k	Wave number of beam wave (=$2\pi/\lambda$).
$\mathbf{K}$	Coloring matrix.
L	Propagation path length.
$\mathbf{L}$	Lower triangular matrix obtained after applying a Cholesky decomposition.
l_0	Inner scale of turbulence.
$n(\mathbf{r})$	Index of refraction.
n_0	Average value of index of refraction.
n_1	Fluctuations of the refractive index.
$\mathbf{Q}$	Orthogonal matrix.
$\mathbf{r}$	Transverse position of observation point.
$U(\mathbf{r}, z)$	Complex amplitude of the field in random medium.
$u_\perp$	Component of the wind velocity transverse to the propagation direction.
$\mathbf{w}[n]$	Coloring Gaussian vector (= $\mathbf{Kz}[n]$).

$\mathbf{z}[n]$	Vector of independent zero mean Gaussian variates with unit variance.
$\alpha_{sc}(t)$	Time-varying atmospheric scintillation sequence.
$\chi(t)$	Log-amplitude fluctuation of scintillation.
$\mathbf{\Lambda}$	Diagonal matrix containing the eigenvalues of $\mathbf{C}_{\chi}$.
ϵ	Turbulent kinetic energy dissipation rate (m^2/s^3).
λ	Wavelength.
$\psi(\mathbf{r}, L)$	Phase perturbations of Rytov approximation.
ρ_{ij}	Normalized cross-correlation coefficient between points i and j in the receiver plane (m).
ρ_l	Degree of randomness as effect of the dynamic evolution of the turbulence ($=\rho_l = \tau_0/\tau_e$).
σ_I^2	Scintillation index (normalized irradiance variance).
σ_{χ}^2	Log-amplitude variance.
τ_0	Turbulence correlation time.
τ_e	Lifetime of turbulent eddies.
$\boldsymbol{\omega}[n]$	Driving noise vector process of an AR model.
$\mathbf{Y}$	Perturbation matrix employed to obtain $\widetilde{\mathbf{C}}_{\boldsymbol{\chi}}$.

10. References

Abramovich, Y. I.; Spencer, N.K. & Gorokhov, A. Y. (2001). Detection-estimation of more uncorrelated Gaussian sources than sensors in nonuniform linear antenna arrays - part I: fully augmentable arrays. *IEEE Transactions on Signal Processing,* Vol. 49, No. 5 (May 2001), pp. 959–971, ISSN 1053-587X.

Alefeld, G. & Mayer, G. (1993). The Cholesky method for interval data. *Linear Algebra and its Applications,* Vol. 194, No.22, (November 1993), pp. 161-182, ISSN 0024-3795.

Al Naboulsi, M. & Sizun, H. (2004). Fog attenuation prediction for optical and infrared waves. *SPIE Optical Engineering,* Vol. 43, No. 2 (February 2004), pp. 319–329, ISSN 091-3286.

Andrews, L. C. & Phillips, R. L. (1998). *Laser Beam Propagation Through Random Media*, SPIE - The International Society for Optical Engineering, ISBN 081942787x, Bellingham, Washington, USA.

Andrews, L. C.; Phillips, R. L. & Hopen, C. Y. (2000). Aperture Averaging of Optical Scintillations: Power Fluctuations and the Temporal Spectrum. *Waves in Random Media,* Vol. 10, No. 1 (2000), pp. 53 – 70, ISSN 1745-5049.

Anguita, J. A.; Neifeld, M. A. & Vasic, B. V. (2007). Spatial correlation and irradiance statistics in a multiple-beam terrestrial free-space optical communication link. *OSA Applied Optics*, Vol. 46, No. 26 (September 2007), pp. 6561–6571, ISSN 1559-128X.

Arnon, S. (2003). Effects of atmospheric turbulence and building sway on optical wireless-communication systems. *Optics Letters,* Vol. 28, No. 2 (January 2003), pp. 129–131, ISSN 0146-9592.

Baddour, K.E.. & Beaulieu, N.C. (2002). Accurate simulation of multiple cross-correlated fading Channels. *IEEE International Conference on Communications (ICC) 2002*, pp. 267–271, ISBN 0-7803-7400-2, New York, NY, USA, April 28 - May 2, 2002.

Beaulieu, N. C. (1999). Generation of correlated Rayleigh fading envelopes. *IEEE Communication Letters*, Vol. 3, No. 6 (June 1999), pp. 172–174, ISSN 1089-7798.

Beaulieu, N. C. & Merani, M. L. (2000). Efficient simulation of correlated diversity channels. *IEEE Wireless Communications and Networking Conference (WCNC 2000)*, Vol. 1, pp. 207–210, ISBN 0-7803-6596-8, Chicago, IL September 2000.

Burghelea, T.; Segre, E. & Steinberg, V. (2005). Validity of the Taylor hypothesis in a random spatially smooth flow. *Physics of Fluids,* Vol. 17, No. 10 (October 2005), art. no. 103101, pp. 103101–103101-8, ISSN 1070-6631.

Campins, J.; Aran, M.; Genovés, A. & Jansà, A. (2007). High impact weather and cyclones simultaneity in Catalonia. *Advances in Geosciences*, Vol. 12, (September 2007), pp. 115–120, ISSN 1680-7340.

Christen, A.; van Gorsel, E. & Vogt, R. (2007). Coherent Structures in Urban Roughness Sublayer Turbulence. *International Journal of Climatology,* Vol. 27, No. 14 (November 2007), pp. 1955–1968, ISSN 1097-0088.

Deutsch, L. J. & Miller, R. L. (1981). Burst Statistics of Viterbi Decoding, In: *The Telecommunications and Data Acquisition Progress Report*, TDA PR 42-64 (May and June 1981), pp. 187-193, Jet Propulsion Laboratory, California Institute of Technology, Pasadena, California.

Ertel, R.B. & Reed, J.H.. (1998). Generation of two equal power correlated Rayleigh fading envelopes. *IEEE Communications Letters*, Vol.2, No.10, (October 1998), pp. 276-278, ISSN 1089-7798.

Fante, R. L. (1975). Electromagnetic Beam Propagation in Turbulent Media. *Proceedings of the IEEE,* Vol. 63, No. 12 (December 1975), pp. 1669–1692, ISSN 0018-9219.

Fried, D.L. (1967). Aperture Averaging of Scintillation. *Journal Optical Society of America,* Vol. 57, No. 2 (February 1967), pp. 169–175, ISSN 0030-3941.

Golub, G.H. & van Loan, C.F. (1996). *Matrix Computations*, The John Hopkins U. Press, ISBN 0-8018-5414-8, Baltimore and London

Haas, S. M.; Shapiro, J. H. & Tarokh, V. (2002). Space-time codes for wireless optical communications. *EURASIP Journal on Applied Signal Processing*, vol. 2002, No. 3 (March 2002), pp. 211–220, ISSN 1110-8657.

Halmos, P.R. (1972). Positive Approximants of Operators. *Indiana University Mathematics Journal,* Vol.21, No.10, (October 1972), pp. 951-960, ISSN 0022-2518.

Hill, R. J. & Frehlich, R. G. (1997). Probability distribution of irradiance for the onset of strong scintillation. *Journal of the Optical Society of America A*, Vol. 14, No. 7 (July 1997), pp. 1530–1540, ISSN 0740-3232.

Holton, G.A. (2004). *Value at Risk: Theory and Practice*, Academic Press, ISBN 978-0123540102, San Diego, USA.

Ibrahim, M.M. & Ibrahim A.M. (1996). Performance analysis of optical receivers with space diversity reception. *IEE Proceedings on Communications,* Vol. 143, No. 6 (December 1996), pp. 369–372, ISSN 1350-2425.

Ishimaru, A. (1997) *Wave Propagation and Scattering in Random Media*, IEEE Press and Oxford University Press, Inc. vol. 1-2, ISBN 0-7803-4717-X, New York, USA.

Juarez, J. C.; Dwivedi, A.; Hammons, A. R.; Jones, S. D.; Weerackody, V. & Nichols, R.A. (2006). Free-Space Optical Communications for Next-Generation Military Networks. *IEEE Communications Magazine,* Vol. 44, No. 11 (November 2006), pp. 46–51, ISSN 0163-6804.

Jurado-Navas, A.; García-Zambrana, A. & Puerta-Notario A. (2007). Efficient lognormal channel model for turbulent FSO communications. *IEE Electronics Letters,* Vol. 43, No. 3 (February 2007), pp. 178 – 180, ISSN 0013-5194.

Jurado-Navas, A. & Puerta-Notario A. (2009). Generation of correlated scintillations on atmospheric optical communications. *OSA Journal of Optical Communications and Networking*, Vol. 1, No. 5 (October 2009), pp. 452–462, ISSN 1943-0620.

Jurado-Navas, A.; Garrido-Balsells, J.M..; Castillo-Vázquez, M. & Puerta-Notario A. (2009). Numerical Model for the Temporal Broadening of Optical Pulses Propagating through Weak Atmospheric Turbulence. *OSA Optics Letters,* Vol. 34, No. 23 (December 2009), pp. 3662 – 3664, ISSN 0146-9592.

Jurado-Navas, A.; Garrido-Balsells, J.M.; Castillo-Vázquez, M. & Puerta-Notario A. (2010). An efficient rate-adaptive transmission technique using shortened pulses for atmospheric optical communications. *OSA Optics Express*, Vol. 18, No. 16 (August 2010), pp. 17346–17363, ISSN 1094-4087.

Jurado-Navas, A.; Garrido-Balsells, J.M.; Castillo-Vázquez, M. & Puerta-Notario A. (2011). A computationally efficient numerical simulation for generating atmospheric optical scintillations, In: Numerical Simulations / Book 2, Editor Dr. Jan Awrejcewicz, InTech, ISBN 978-953-307-1423-5, Vienna, Austria.

Jurado-Navas, A.; Garrido-Balsells, J.M.; Paris, J. F. & Puerta-Notario A. (2011). A unifying statistical model for atmospheric optical scintillation, In: *arXiv:1102.1915v1 [physics.optics]*, February 2011, Available from: http://arxiv.org/abs/1102.1915. An extended version to appear in: Numerical Simulations / Book 2, Editor Dr. Jan Awrejcewicz, InTech, ISBN 978-953-307-1423-5, Vienna, Austria.

Kay, S. M. (1988). *Modern Spectral Estimation: Theory and Application*, Prentice-Hall, ISBN 013598582x, Englewood Cliffs, NJ.

Lee, E. J. & Chan, V. W. S. (2004). Part I: Optical communication over the clear turbulent atmospheric channel using diversity. *IEEE Journal on Selected Areas in Communicactions*, Vol. 22, No. 9 (November 2004), pp. 1896–1906, ISSN 0733-8716.

Mercier, F.P. (1962). Diffraction by a Screen Causing Large Random Phase Fluctuations. *Mathematical Proceedings of the Cambridge Philosophical Society,* Vol. 58, No. 2 (April 1962), pp. 382–400, ISSN 0305-0041.

Monserrat, J.F.; Fraile, R. & Rubio, L. (2007). Application of alternating projection method to ensure feasibility of shadowing cross-correlation Models. *IET Electronics Letters,* Vol. 43, No. 13 (June 2007), pp. 724–725, ISSN 0013-5194.

Moore, C. I.; Barris, H. R.; Stell, M. F.; Wasiczko, L.; Suite, M. R.; Mahon, R.; Rabinovich, W. S.; Gilbreath, G. C. & Scharpf, W. J. (2005). Atmospheric turbulence studies of a 16 km maritime path. *Proceedings of SPIE: Atmospheric Propagation II*, SPIE, Vol. 5793, Orlando, FL, pp. 78–88, ISSN 9780819457783.

Muhammad, S.S.; Kohldorfer, P. & Leitgeb, E. (2005). Channel modeling for terrestrial free space optical links. *Proceedings of 2005 7th International Conference on Transparent Optical Networks,* IEEE, Barcelona, Spain, pp. 407–410, ISBN 0-7803-9236-1.

Papoulis, A. (1991). *Probability, Random Variables, and Stochastic Processes* (3rd edition), McGraw-Hill, ISBN 0070484775, New York, USA.

Razavi, M. & Shapiro J.H. (2005). Wireless optical communications via diversity reception and optical preamplification. *IEEE Transactions on Wireless Communications,* Vol. 4, No. 3 (May 2005), pp. 975–983, ISSN 1536-1276.

Strohbehn, J.W. (1968) Line-of-Sight Wave Propagation through the Turbulent Atmosphere. *Proceedings of the IEEE*, Vol. 56, No. 8, (August 1968), pp. 1301–1318, ISSN 0018-9219.

Strohbehn, J.W. (1971) Optical Propagation through the Turbulent Atmosphere. in *Progress in Optics*, Vol. 9, pp. 73 – 122, ISBN 0720415098, edited by E. Wolf (North-Holland, Amsterdam, 1971).

Strohbehn, J.W. (1978)*Laser Beam Propagation in the Atmosphere*, Springer, Topics in Applied Physics Vol. 25, ISBN 3-540-08812-1, New York, USA.

Strohbehn, J.W. & Clifford, S.F. (1967) Polarization and Angle-of-Arrival Fluctuations for a Plane Wave Propagated through a Turbulent Medium. *IEEE Transactions on Antennas and Propagation*, Vol. 15, No. 3 , (May 1967), pp. 416–421, ISSN 0018-926X.

Tatarskii, V. I. (1971). *The Effects of the Turbulent Atmosphere on Wave Propagation*, McGraw-Hill, ISBN 0 7065 06804, New York, USA.

Taylor, G.I. (1938). The Spectrum of Turbulence. *Proceeding of the Royal Society of London. Series A, Mathematical and Physical Sciences,* Vol. 164, No. 919 (February 1938), pp. 476–490.

Willis, G.E. & Deardorff, J. W. (1976). On the use of Taylor's hypothesis for diffusion in the mixed layer. *Quarterly Journal of the Royal Meteorological Society,* Vol. 102, No. 434 (October 1976), pp. 817 – 822, ISSN 0035-9009.

Zhu, X. & Kahn, J.M. (2002). Free-space optical communication through atmospheric turbulence channels. *IEEE Transactions on Communications*, Vol. 50, No.8, (August 2002), pp. 1293-1300, ISSN 0090-6778.